MechanoBeat: Monitoring Interactions with Everyday Objects using 3D Printed Harmonic Oscillators and Ultra-Wideband Radar

Md Farhan Tasnim Oshim[1], Julian Killingback[1], Dave Follette[2], Huaishu Peng[3], Tauhidur Rahman[1]

[1]College of Information and Computer Sciences
University of Massachusetts Amherst
{farhanoshim, jkillingback, trahman}@cs.umass.edu

[2]Institute for Applied Life Sciences
University of Massachusetts Amherst
follette@umass.edu

[3]Computer Science
University of Maryland, College Park
huaishu@cs.umd.edu

Figure 1. MechanoBeat uses (a) different electronics-free harmonic mechanical oscillator designs on everyday objects like (b) a pill bottle to automatically generate different unique mechanical heartbeat signals. At the moments of (b) user-object interaction, MechanoBeat tags generate unique mechanical heartbeats which are illustrated in the form of a radargram (c) An ultra-wideband radar array scans the living space and can reliably detect the unique mechanical heartbeat in both line-of-sight and non-line-of-sight conditions (e.g., through walls).

ABSTRACT

In this paper we present MechanoBeat, a 3D printed mechanical tag that oscillates at a unique frequency upon user interaction. With the help of an ultra-wideband (UWB) radar array, MechanoBeat can unobtrusively monitor interactions with both stationary and mobile objects. MechanoBeat consists of small, scalable, and easy-to-install tags that do not require any batteries, silicon chips, or electronic components. Tags can be produced using commodity desktop 3D printers with cheap materials. We develop an efficient signal processing and deep learning method to locate and identify tags using only the signals reflected from the tag vibrations. MechanoBeat is capable of detecting simultaneous interactions with high accuracy, even in noisy environments. We leverage UWB radar signals' high penetration property to sense interactions behind walls in a non-line-of-sight (NLOS) scenario. A number of applications using MechanoBeat have been explored and the results have been presented in the paper.

UIST '20, October 20–23, 2020, Virtual Event, USA

ACM ISBN 978-1-4503-7514-6/20/10 $15.00.
https://doi.org/10.1145/3379337.3415902

Author Keywords

Mechanical Oscillator Tag, 3D Printing, Contactless Sensing, User-Object Interaction, Ultra-Wideband Radar

CCS Concepts

•Human-centered computing → Ubiquitous and mobile computing systems and tools;

INTRODUCTION

Knowing how and when people interact with their surroundings is crucial for constructing dynamic and intelligent environments. Despite the importance of this problem, there still lacks an attainable and simple solution. Current solutions often require powered sensors on monitored objects or users themselves. Many such systems use batteries, which are costly and time consuming to replace. Some powered systems connect to the grid which may save swapping batteries, but at the price of restricted placement options. Other solutions use passive tags on monitored objects or require no tags at all, but many of these systems have prohibitive characteristics. For

instance, camera based systems generally will not work if their view is occluded. Many other systems that rely on passive tags or do not use tags require direct line-of-sight or close proximity to work.

Previous approaches not only have significant drawbacks and constraints in their use and operation, but also in their cost. Even the most affordable electronic tags, that use inexpensive analog components, cost several dollars to produce; putting them out of reach for liberal use in many environments.

As such, our goal was to design and develop small, cheap, easy-to-install tags that do not require any batteries, silicon chips or discrete electronic components, and which can be monitored without direct line-of-sight.

In this paper, we propose *MechanoBeat*, which provides a solution that leverages the sensing capabilities of ultra-wideband (UWB) radar to detect harmonic oscillations produced by ultra low cost tags. MechanoBeat uses unique harmonic oscillations or "heartbeats" as tags. These tags can be mounted on various stationary or movable objects and are monitored remotely by UWB radar boxes which sense when a tag is activated.

To our knowledge, no other research has explored using harmonic oscillation as a tagging mechanism in conjunction with UWB radar. Here we investigate the limitations of UWB radar to detect and classify harmonic oscillation.

We explore various oscillation based tag designs that allow for both stationary and mobile use cases. All of our tags can be printed on hobbyist grade 3D printers using various plastic filaments and can easily be adapted for injection molding. Our proposed tag designs can be manufactured for well below a dollar and require no power and minimal maintenance.

The proposed tags can be classified into two categories: stationary tags and mobile tags. Stationary tags can be used to detect interactions with stationary objects, for instance, kitchen appliances (freezers, microwaves, cabinets, drawers, etc.), washing machines, water faucets, and so on. These interactions are important for creating life logs, smarter homes, smarter workplaces, and potentially facilitate ambient assisted living. On the other hand, mobile tags can be attached to pill bottles, sugar jars, water bottles, etc., to track individuals' medication routines, sugar intake, and hydration status, respectively.

To find when and where tags are activated we develop a deep learning classification pipeline which takes radar data as input and outputs the tags that are currently active. We show empirically that our pipeline is robust to environmental noise and capable of inferring tag activity even when the radar is obscured. Furthermore, we demonstrate the versatility of our deep learning pipeline to detect a variety of tags in many potential use cases.

RELATED WORKS

Object-Interaction in Indoor Environments

Recognizing interactions with different objects in an indoor environment has been and continues to be an active area of research. Several approaches have been proposed to tag different everyday objects and to recognize when and how a user interacts with them. The most straightforward being, placing powered digital sensors directly on a given object, or on the user's body [22, 30, 33, 27]. Such approaches have the benefit of potentially improved accuracy resulting from direct contact and minimal additional setup, but at the expense of obtrusiveness, affordability, and maintainability. Commercial sensors can often be costly [5, 29, 18]. Moreover, battery powered sensors require their batteries to be changed, adding to the cost and complexity of operation.

To circumvent the problems associated with battery-powered sensors, some tags piggyback on the existing power infrastructure of the environment to harvest energy [46]. For instance, PowerBlade [11] uses harvested energy from the electrical plug that it sits on. Another example, Sozu, uses power generated from the use of the object that was tagged, to generate a RF chirp that is then picked up by a remote hub [43]. Similar to RFID, Sozu harvests a bit of energy through a different power harvesting mechanism and transmits a signal with that energy to a base station. Such approaches do remove the need for battery changes, but requires electronics to be deployed in different target locations.

Object-borne sensors can be very accurate, but their cost and maintenance implications have spurred research into sensors that can detect many object interactions in a wide area. Such sensors are often centrally located and have access to power, making them quick to set up in a large area, often cheaper than on-object sensors, and easier to maintain. Such systems may still have tags that are placed on objects, but generally the tags require no power and are not functional without the main sensor's input.

One wide-area approach is to use a camera based system to determine how and when an object is interacted with [21, 25]. However, this approach is fraught with privacy concerns (especially for home deployment) and suffers from strict line-of-sight requirements. Another popular approach leverages existing infrastructure for wide range sensing. These approaches have utilized, plumbing [13, 14], gas lines [8], HVAC [31], and electrical systems [9, 17, 32] within interiors to find how individuals interact with objects and their environment. Other efforts for wide-area sensing have used, laser vibrometry [44], EMI antennas [45], and multi-sensor-fusion boards [23] to achieve high accuracy large-area sensing. Vibrosight [44] for instance, used a laser vibrometry sensor that requires direct line-of-sight to sense the interaction with tags, whereas user interaction with our proposed MechanoBeat can be discovered with a UWB radar array which does not require any line-of-sight and can detect tags from behind obstacles like wood, brick walls, etc. [39, 4].

Sensing with RF Signals

Sensing with RF signals has received significant attention from the research community. Different parts of the RF and microwave spectrum have been explored with radar, software defined radio, and commercially available WiFi transceivers for different sensing applications including indoor localization and tracking [41, 3, 16], room occupancy monitoring [7, 28], vital sign monitoring [24, 35], activity recognition [20, 47]), and sleep monitoring [34]. Building on the existing literature,

we use a UWB radar array for monitoring interaction with everyday objects. UWB radar offers several advantages over other radar architectures including FMCW radar. For example, due to the narrow pulse duration and high update rate, the UWB offers higher range resolutions specially for moving objects compared to FMCW radar [12]. Thus, UWB radar enables us to detect subtle harmonic oscillations of our tags.

Another approach to wide-area sensing uses backscatter technology such as Wi-Fi for sensing interaction with different objects. This technique uses passive tags, such as RFID or 3D printing wireless connected objects [23, 19, 6, 42, 36]. However, these 3D printed wireless connected objects [19], require printing backscatter antennas and switches in order to encode and transmit interaction data to the receiver. These antennas and switches are object specific, such as a detergent flowmeter, anemometer, scale, etc. which are not necessarily reusable and incur significant cost in the instrumentation process. Aircode [25] and Infrastructs [38] both embed tagging information in the fabrication process and read the tag through computational imaging or terahertz imaging methods respectively. The former requires line-of-sight imaging to reach the embedded tags, while the latter has better penetration capability but more expensive transmitters and receivers.

On the other hand, our proposed MechanoBeat is reusable and scalable allowing it to be attached to nearly any stationary or movable object. Unlike the above-mentioned approaches, in this study, we aim to develop an electronics-free tag based on low-cost, 3D printable harmonically oscillating objects. Upon user interaction, the attached tag triggers a unique mechanical oscillation that can be detected with a UWB radar array even in the presence of human movement or other vibrating objects.

MECHANOBEAT: SYSTEM OVERVIEW

Design considerations

Before explaining our technical approach, let us discuss a few specific design considerations that went into the development of the MechanoBeat tag and sensor system.

- In this study, we aimed to design and develop a low burden mechanism for recognizing interactions between humans and everyday objects with simple, low-cost tags and contactless sensors.

- We required the tags to trigger a specific oscillation pattern with unique spectral characteristics at the moment of human-object interaction for a short period. Moreover, a reset mechanism can mark the end of the interaction and allow differentiation between two consecutive interactions with the same object.

- Our goal was to make low-cost tags with small form factors that are scalable. Commodity desktop 3D printers offer readily scalable solutions for printing mechanical tags with cheap materials. The tags should be compatible and easily attachable to different everyday objects of interest. Lastly, the tags should be durable and reusable which can provide us with a sustainable and a long-lasting human-object interaction tracking solution.

- The sensing system should not require additional instrumentation of the user's body. The system should be able to detect active tags during human-object interaction in noisy and real-world conditions. Most importantly, in a real-world setting, there is no guarantee that a direct line-of-sight can be established between the sensor and the tags. Thus, our system should be able to have high accuracy even when the tags are obscured (non-line-of-sight scenario).

Based on these design considerations, we aimed to design, develop, and validate an approach that uses electronics-free 3D printable simple mechanical oscillators along with a UWB radar-based contactless sensor array. MechanoBeat leverages the P440 UWB radar operating at 3.1-4.8 GHz frequency that can see through different objects and detect human-object interactions happening behind a wooden or cardboard partition and even behind walls. We leverage multiple UWB radar units placed at different locations to observe human-object interactions from multiple points of view. The complementary signals are then fused to achieve better detection accuracy.

MechanoBeat Tag: Harmonic Oscillator

The simple harmonic oscillator designs that we explored in this paper as MechanoBeat tags can broadly be classified into two types: stationary and mobile tags. The stationary tags are appropriate for tagging stationary objects such as a drawer, door, or cabinet. On the other hand, the mobile tags can be used to tag objects that move with the user such as a pill bottle, water bottle, or a sugar jar.

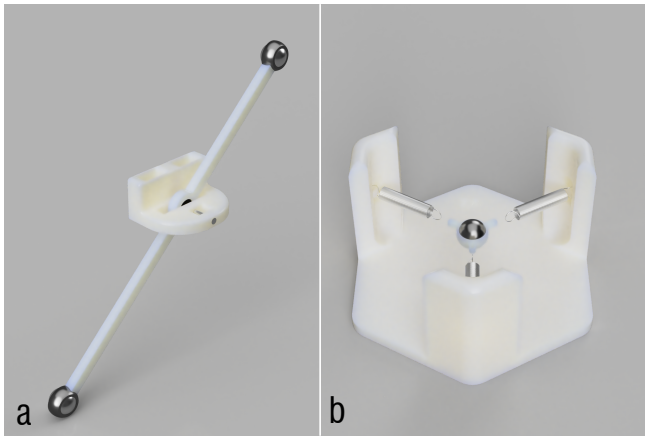

Figure 2. Stationary tag design: (a) pendulum based tag (b) linear spring-mass tag.

Stationary Tags: Since the user-object interaction mechanism for stationary objects (e.g., a drawer is opened and closed

$T = 2\pi\sqrt{\frac{I}{gY}}$	*Single Ball*					*Double Ball*				
Version	*A*	*B*	*C*	*D*	*E*	*F*	*G*	*H*	*I*	*J*
Long Arm (mm)	40	60	80	28	42	40	60	80	100	100
Short Arm (mm)	0	0	0	0	0	28	42	56	70	80
Gravity Ratio (γ)	1	1	1	1	1	0.3	0.3	0.3	0.3	0.2
Frequency (Hz)	2.5	2.0	1.8	3.0	2.4	1.4	1.1	1.0	0.9	0.7

Table 1. Different combinations of arm lengths to generate different frequencies for pendulum based tag.

by applying outward or inward horizontal force) does not change over time, simple oscillators including a pendulum and a spring-mass can be used with an easy mounting technique. Another advantage is that once these simple tags are mounted to a fixed location, the direction of gravity does not change over time. As a result, simple tags that are comprised of a pendulum or spring mass oscillator maintain their periodic cycles. Figure 2(a) shows a pendulum-type tag design which includes two arms with length l. To tag multiple objects with this pendulum design, we need a scalable approach to design unique oscillation frequencies. To this end, we can either use a single ball option by attaching a weight to the lower arm and keeping the other arm free, or we can have a double ball option with weights at both arms. Both options offer unique oscillation frequencies. Table 1 illustrates examples of different pendulum-based tags and associated design parameters to produce unique frequencies in the range of 0.7 Hz to 3 Hz. The oscillation frequency is calculated as the inverse of the time period found in $T = 2\pi\sqrt{\frac{l}{g\gamma}}$. The gravity ratio γ comes into play when we create a double ball tag with different arm lengths and can be calculated as $(long - short)/long$. This factor reduces the effect of gravity and increases the length of the period causing lower oscillation frequencies for tags with weights in two arms compared to the single ball option. Pendulum-based tags with both a single ball and double balls provide us with the opportunity to create distinguishable tags in a variety of oscillation frequencies.

Figure 2(b) shows another stationary tag, a linear spring-mass design (upside down). We attach a magnet to the bottom of the object we want to interact with (pill bottle, sugar jar, water bottle, etc.) and place it on top of the tag. The metallic ball at the center of three springs will be attracted to the top. The tag activates when the object is taken off the surface of the tag, causing the metal ball to oscillate at a unique frequency determined by the spring constant (k) and mass (m) of the ball ($T = 2\pi\sqrt{\frac{m}{k}}$). Using different springs with varying spring constants we can design more tags for large scale use.

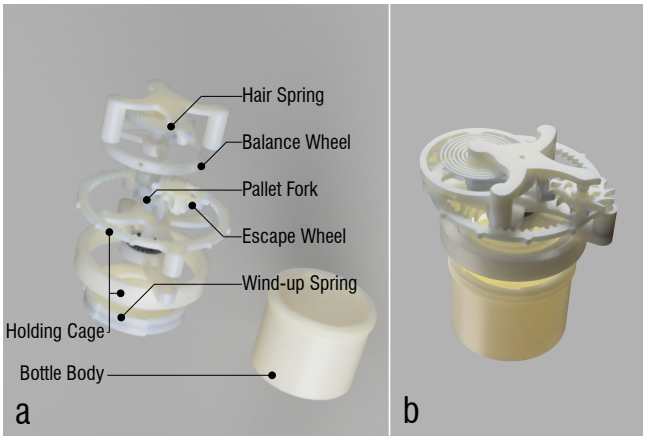

Figure 3. Mobile tag design: (a) tourbillon bottle tag explosion view and (b) assembly view.

Mobile Tags: Although pendulum and spring-mass tags are reliable for stationary setups, they are not robust to mechanical disturbances such as a sudden change of position or orientation. Thus, they are not suitable for mobile settings where the tagged object may shift its 3D location in the environment.

Our mobile tag draws great inspiration from a tourbillon design, which has been used in mechanical watches for centuries to maintain accuracy against drag due to gravity. A basic tourbillon design (Figure 3a) has a holding cage, a wind-up spring, and a core revolving structure including a balance wheel, a pallet fork, an escape wheel, and a hairspring. The balance wheel is the "beating heart" of the tourbillon, which is analogous to the pendulum or spring-mass in the stationary tag design. It oscillates around its axis and is regulated by the connected hairspring. The key to the tourbillon design is to make the balance wheel revolve around the central axis of the entire holding cage, canceling the applied gravity effect. This is achieved by connecting the balance wheel to an escape wheel via a pallet fork. While the balance wheel oscillates on its own axis, the rotational motion is transmitted to the escape wheel which drives the entire core structure to revolve around the holding cage, one tick at a time. The energy of the constant ticking motion is from the wind-up spring. Figure 3(b) shows our design which integrates a printed tourbillon tag (based on Thingiverse Thing ID: 2751917) to a threaded pill bottle lid. The tourbillon's holding cage serves as the bottle lid and the wind-up spring can be fixed to the inner wall of the bottle body when the bottle lid is put on. When the lid is opened or closed, the twisting motion of the lid will wind the spring, driving the tourbillon to revolve. Note that different unique oscillation frequencies can be ensured by adjusting the balance wheel, the hairsprings, and the ticking steps of the escape wheel.

MechanoBeat Sensor: UWB Radar

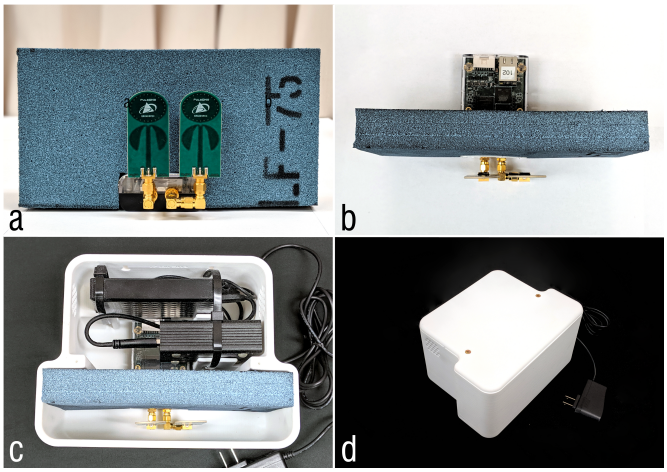

Figure 4. (a) P440 MRM radar module with an absorber behind the antenna. (b) Top view of the radar with an absorber. (c) Radar Box with Raspberry Pi and a hard disk drive. (d) Enclosed radar box.

MechanoBeat uses PulsON 440 (P440) ultra-wideband radar in monostatic mode [1]. The operating frequency of the radar ranges from 3.1 to 4.8 GHz with the center frequency at 4.3 GHz. Due to wide bandwidth and therefore extremely short pulse duration (nanosecond level), UWB radars have very high range resolutions which make them appropriate for fine-grain sensing applications like monitoring vitals signs and sensing harmonic oscillations. As shown in Figure 4(a), the P440

unit has a transmitter and a receiver antenna. To scan a target living space, the transmitter antenna repeatedly transmits a low energy, short-duration impulse signal which gets reflected by different stationary objects (e.g., furniture and other static clutter), moving objects (e.g., MechanoBeat tags, fan), and the human body. The backscattered impulse signal is received by the receiver antenna and the time-of-flight (ToF) of these received pulses is estimated from the round-trip propagation delay, which is then used to calculate the target's distance by multiplying with the speed of light. The backscattered impulse signal from multiple scans is stacked together to form a two-dimensional radargram which is used to detect the oscillation of different active MechanoBeat tags. Figure 5 illustrates a sample radargram signal in the form of an image. The oscillating pendulum-based MechanoBeat tag was placed at a distance of roughly one meter from the radar which corresponds to the 55^{th} range bin. Here, the horizontal axis indicates the distance or range bin number, also known as the fast time. Along the vertical axis from top to bottom, the scan number increases. This axis is also known as slow time (in seconds). The raw radargram signal captures reflections from all the objects (both moving and stationary) at different distances or ranges. Since our living spaces are primarily made of stationary objects and the reflections from the stationary objects do not change across different scans, we can observe vertical lines in the radargram. However, if we observe closely (between the onset and the end of oscillation in Figure 5), we can see periodic changes due to the active MechanoBeat tag.

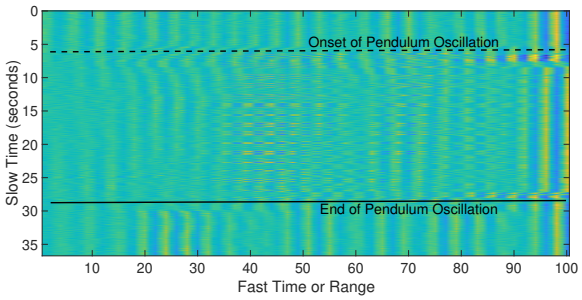

Figure 5. Radargram of a pendulum-based MechanoBeat tag oscillation.

The radar antennas are omnidirectional, so a microwave absorbing material of dimension 8.5" × 4.5" × 1.13" is placed at the back of the antennas to attenuate the signals from behind the radar. The absorber material we used is a commercially available *LF*75 absorber which provides attenuation of -20 dB for a frequency range of 2.5 GHz to 40 GHz. The PulsON 440 UWB radar unit, the absorber material, a Raspberry Pi unit, and a hard disk drive to store the data locally are placed in a 3D printed T shaped box as shown in Figure 4(b-d). The radar data collection program written in C, is run on the Raspberry Pi in the background and stores each minute of data locally with corresponding timestamps.

MechanoBeat Sensing Pipeline

The sensing pipeline starts from the radargram data (as shown in Figure 5) which contains reflections from both stationary (e.g., walls, furniture) and moving objects (e.g., MechanoBeat tags, fan, human movements) in the living space. Each column of the radargram matrix can be considered as a time series signal corresponding to a single range bin. This time domain signal contains reflection information from different stationary and moving objects at that particular range bin. To get rid of the stationary components as well as the unwanted higher frequency oscillation from different machines or appliances (e.g., fan or air-conditioner), we apply a bandpass IIR filter on the time domain signals of each range bin across different scan numbers or slow time. Thus, the filtered radargram only preserves the operating frequency range of the tags and removes all undesirable frequencies.

To train a user-object interaction classifier based on the tag frequency, first we window the radargram signal across the slow time or scans. Instead of using all the range bins, we focus on a specific window of range bins (i.e., focus range region). Since each tag is located in a small portion of the range covered by the radar and the tag's oscillation signal is subtle in nature, focusing on a window of range bins allows the subtle tag frequency to be preserved. Moreover, similar to the windowing across slow time which allows the classifier to detect an active tag over time, the windowing across fast time or range allows the classifier to automatically locate the position of the tag. Now, to develop the classifier, we have explored both the traditional machine learning approach with manual feature engineering and the deep learning approach.

Modeling with Traditional ML approach

From the temporally filtered and windowed radargram, we extract the time aligned 1D signal as well as individual 1D time series signals associated with a few specific range bins. The time-aligned 1D signal is extracted by aligning the temporal signals for each range bin (based on correlation) and summing up the signals. The individual time series are extracted from the central range bin of the focused range region as well as N range bins in either direction of the central bin. While the 1D time aligned signal tries to capture the overall oscillations that are prevalent in the focus range region, the 1D time series at specific range bins can capture variabilities in oscillations across different parts of the focus range region. We apply a fast Fourier transformation (FFT) on each of the 1D time series signals and estimate the frequencies corresponding to the highest and second highest peaks to estimate the most dominant periodicities in the signal. We also estimate the zero crossing rate of each of the 1D signals as a measure of noisiness. Lastly, we train different traditional machine learning algorithms including random forest, K nearest neighbors, and support vector machines. Random forest consistently outperformed the rest of the classifiers that we considered.

Modeling with Deep Learning approach

As single range bin inputs have only one dimension, time, we adopted a one dimensional convolution neural network (1D CNN) architecture. Our 1D CNN model has a total of six 1D convolutional layers. Each layer contains 64 kernels, uses a ReLU activation function, and has a stride length of 1. The convolutional layers are split into two sections that are separated by a mean pool layer. The first section has kernels of length 3, 5, and 7. The mean pool layer has a pool size of 2 and a stride length of 2. The second section has kernels of

length 9, 13, and 27. After the second convolutional section, there is a second mean pool with a size of 2 and stride of 2. Then a flatten layer followed by a fully connected layer with a ReLU activation function and size 128. Finally, a fully connected prediction layer with a softmax or sigmoid activation function and a size equal to the number of classes. We use softmax for all experiments except the multiple tag classification experiment where we use sigmoid. The loss is categorical cross entropy for all experiments except for multi-tag classification where the loss is binary cross entropy. For all experiments, the optimizer is Adam using the default parameters in TensorFlow.

A minimal stride length is used to preserve as much information as possible in each layer. We found that 64 kernels gave us minimal overfitting while still providing low validation and test loss. In order to reduce further over-fitting, we introduced spatial dropout with a drop out rate of 0.1 between the first and second convolutional layers as well as a spatial dropout with a drop out rate of 0.05 between the second and third convolutional layers in both convolutional sections.

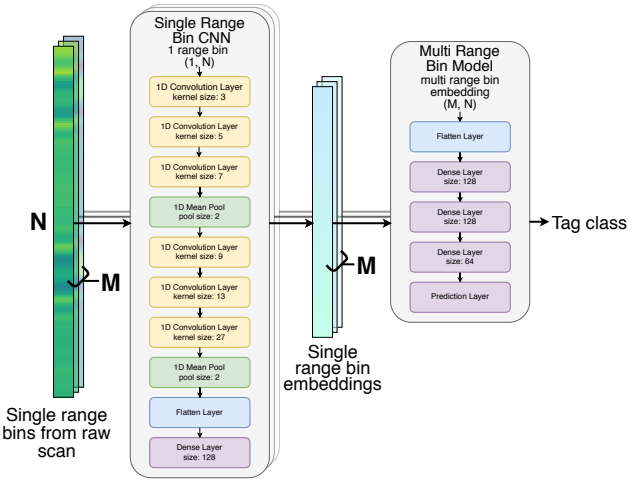

Figure 6. Deep learning classification pipeline.

Input is a single range bin for a given time window of length N. The small time window allows the model to detect short lived oscillations enabling greater freedom in tag design and future applications. After the single range bin model is trained the prediction layer is removed and all layers are frozen. At this point the model outputs an embedding of length 128 for each range bin inputted. The embedding for each range bin in a given time window is then combined to get a $128 \times M$ embedding for the whole time window.

The second step of our deep learning pipeline takes a $128 \times M$ embedding as input and outputs the final tag class. For this step a simple fully connected neural network model is used, which we will refer to as the mutli-range bin model. The first layer in the model is a flatten layer, followed by three dense layers of size 128, 128, and 64 each with a ReLU activation function. Between each of these layer is a dropout layer with a drop out rate of 0.1. The final layer is a prediction layer with a softmax activation function and a size equal to the number of classes. The loss for the multi-range bin model is categorical cross entropy and the optimizer is Adam using the default parameters in TensorFlow.

PROOF-OF-CONCEPT EXPERIMENTS WITH SIMPLE HARMONIC MECHANICAL OSCILLATOR

For the initial proof of concept of our idea, we ran a series of experiments with two different simple harmonic oscillators as shown in Figure 7: (a) spring-mass and (b) pendulum.

Experimental Setup

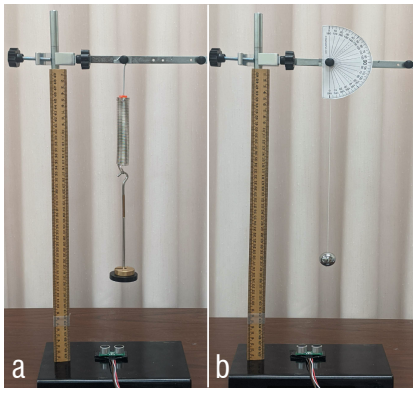

Figure 7. (a) Spring-mass and (b) pendulum oscillator.

Mass	*Frequency (rpm)*	*String length*	*Frequency (rpm)*
80 g	160	10 inch	59.7
100 g	144	12 inch	54.8
130 g	128	14 inch	50.7
160 g	116	16 inch	47.5

Table 2. Oscillation frequencies in rotations per minute (rpm) (left) for different spring-mass oscillators with different mass and a spring constant of 5N/m and (right) for different pendulum frequencies for different string lengths.

Experiment 1: Spring-Mass Oscillator

For the first proof of concept experiment, we set up a simple spring-mass oscillator where the frequency of oscillation is determined by the mass attached to the spring. We used a single spring with a spring constant of 5 N/m and varied the mass. As shown in Table 2 (left), different oscillation frequencies can be generated simply by changing the mass weights.

We employed two radars on two adjacent walls to sense the oscillation. The spring-mass setup was placed at a distance of one meter from each radar. In a noise-free setting, we could detect the peak frequencies of oscillation for all the spring-based tags in the frequency domain after performing time alignment and FFT. Figure 8 (left) shows the frequency peaks detected for different spring-based tags which closely matches with the theoretical frequencies in Table 2 (left).

We also employed frequency-based feature extraction and applied machine learning on the collected spring tag oscillation data with a window size of 10 seconds and a shift of 0.5 seconds. With no external noise, our detection algorithm using random forest classification resulted in 98% accuracy and an

F1 Scores of 0.98 for Radar 1 and 93% accuracy with an F1 score of 0.94 for Radar 2.

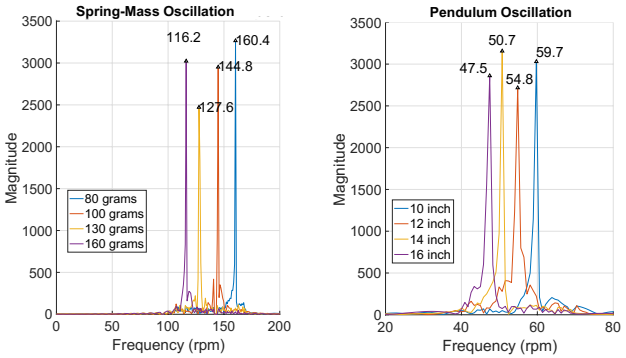

Figure 8. Estimation of the fundamental frequency of (a) (left) different spring-mass oscillations and (b) (right) pendulum oscillations in noise-free setting.

Experiment 2: Pendulum-based Oscillator

The second type of simple harmonic oscillator we used is the pendulum with which we set up the same experiment as experiment 1. Table 2 (right) shows that by changing the string lengths, one can change the frequency of the oscillation. Figure 8 (right) shows the frequency peaks detected for different spring-based tags which closely match with the theoretical frequencies presented in Table 2 (right). In a noise-free condition, the pendulum tag is detected by a random forest classifier with an 88.76% F1 score.

Experiment 3: Window Size Test

Window size can have a significant impact on the tag classification. Since practical harmonic mechanical oscillators can produce reasonably short-lived oscillation (due to friction), a classifier that can accurately detect the active mechanical tags with a short time window is desirable. On the other hand, a short time window from the radar's signal contains only a few oscillation cycles which increases the likelihood of a low signal to noise ratio (SNR).

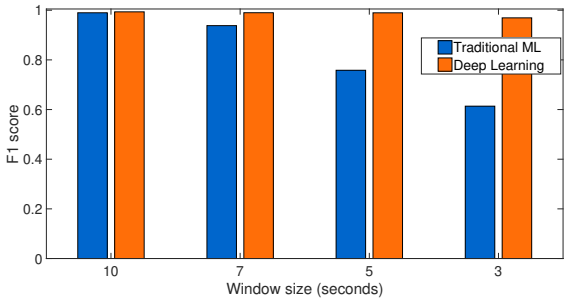

Figure 9. shows the performance of traditional ML and DL approaches in terms of F1 score across different window sizes.

In this experiment, we evaluated the performance of both the traditional ML model (i.e., random forest) and the deep learning model (i.e., 1D CNN) with multiple window sizes. As seen in Figure 9, both random forest and 1D CNN models perform highly at the window size of 10 seconds. However, as the window size became smaller, our 1D CNN model continues to have high performance while the performance of random forest decreases sharply. With the window size of 3 seconds, our deep learning approach achieved an F1 score of 0.9693. Since a model operating at a smaller window size has the advantage of better detecting short lived oscillations and can more precisely find the transition from an oscillating tag to a stopped tag, we opted for the 1D CNN model for this study. From this point on, we will only report the results of the 1D CNN model.

Experiment 4: With External Noise

This experiment was performed to test the robustness of the 1D CNN model in the presence of different external noises. To add external noise, we introduced different human activities as well as electromechanical machines close to the active harmonic oscillators. The human activities include walking, typing, and repeatedly moving hands. We also used a pedestal fan close to the active harmonic oscillators to introduce machine noise. The four spring-mass and four pendulum frequencies outlined in Table 2 were used in the presence of each of these external noises.

Table 3 and Table 4 show the performance of 1D CNN-based harmonic oscillator classification model with two different window sizes (i.e., 3 seconds and 5 seconds). With a window size of 3 seconds, the classifier performs moderately well across different noise categories. The performance of the classifier was at it's lowest with hand motion because any random hand motion can degrade the quality of a 3-second long window significantly. However, with a slightly larger window size of 5 seconds (Table 4), the 1D CNN achieved better performance across all the noise settings. The longer window captured more periods of the oscillation which increased the SNR.

Metric/Noise	*Noise Free*	*Hand Motion*	*Walking*	*Fan*	*Typing*
Precision	0.9695	0.7064	0.8960	0.8013	0.9053
Recall	0.9690	0.7026	0.8953	0.8012	0.9043
F1 score	0.9693	0.7045	0.8957	0.8012	0.9048

Table 3. Performance of tag classification with different introduced noise with DL approach for a window size of 3 seconds

Metric/Noise	*Noise Free*	*Hand Motion*	*Walking*	*Fan*	*Typing*
Precision	0.9897	0.8785	0.9441	0.9079	0.9739
Recall	0.9897	0.8717	0.9429	0.9039	0.9709
F1 score	0.9897	0.8751	0.9434	0.9059	0.9724

Table 4. Performance of tag classification with different introduced noise with DL approach for a window size of 5 seconds

Experiment 5: Displacement Test

In this experiment, we investigate what the minimal level of displacement a harmonic oscillator should generate for it to be reliably detected by our radar and classifier. The oscillator displacement can be measured by the peak-to-peak distance between two extreme positions of the oscillation. To this end,

we started a spring-mass oscillator and allow it to oscillate for a long period (i.e., 1 hour) until the oscillation becomes almost invisible. The spring-mass tag with an attached mass of 160 grams and a 5 N/m spring constant was left to oscillate at 116 rpm. An ultrasonic distance sensor was placed at the base for measuring the distance of the mass from the bottom.

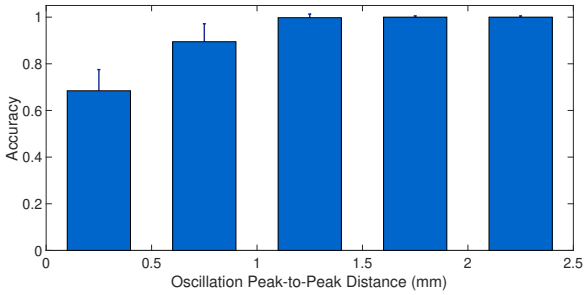

Figure 10. Tag frequency estimation accuracy at different oscillation peak-to-peak distance values.

Figure 10 shows that at a higher peak-to-peak distance the oscillation could be detected reliably by our system. However, as the peak-to-peak distance goes below 1 mm, the oscillation detection accuracy of our classifier lowers significantly. For a certain oscillation to be visible to our UWB radar and 1D CNN based system, the minimum displacement has to be at least 1 mm. Comparing the minimum displacement (1 mm) with the range resolution of the UWB radar (9 mm), we can see that MechanoBeat is achieving sub-pixel level oscillation resolving capability. In recent work on video motion magnification, we can see how an algorithm captures sub-pixel level oscillation information [26, 10]. Lastly, we also ran the random forest model on this data and found that it failed to reliably discover oscillation which produces less than 3.048 mm of peak-to-peak displacement.

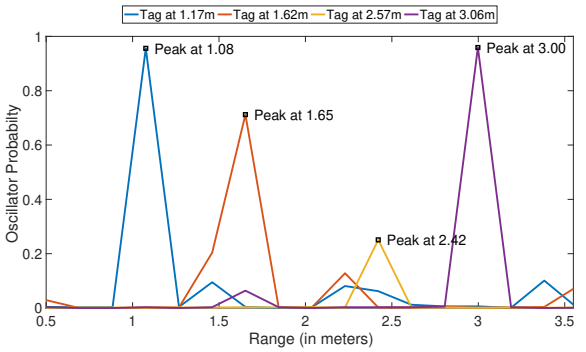

Figure 11. Detecting active harmonic oscillator at multiple distances.

Experiment 6: Detecting Oscillation across Multiple Locations

In the previous experiments, we assumed that we know the location of the harmonic oscillators and our 1D CNN model extracts oscillation information from $Location \pm N$ range bins (N is typically less than 50). In this experiment, we aim to explore whether the proposed harmonic oscillation detection scheme works across multiple locations. We trigger a spring-mass oscillator at four different locations in a living space which results in four radargram recordings. We sweep the focus range of our 1D CNN model across the entire range to detect the oscillation and associated probabilities at multiple locations. Figure 11 shows the probability of a certain tag across the entire range of the radar. For each of the locations (mentioned in the legend), we can see the probability value peaks at a close-by range value. This experiment shows that the MechanoBeat system is able to scan the entire room and find the activated (oscillating) tag in a room when the location of the tag is unknown. By using multiple UWB radar units and by inferring the activated tag locations, we can identify the locations of the activated tags over a two-dimensional space (further details in Figure 18).

Experiment 7: How many Tags can we detect?

A number of factors play a role in determining the number of tags that can be reliably detected by our system. Oscillation frequency is the key distinguishing factor, other than location, for each tag; thus, we wanted to know what range of frequencies we can reliably detect. The upper bound for this range broadly depends on the sampling frequency of the UWB radar hardware, which in turn depends on the configured maximum range of the UWB radar. As our experiments are performed in a small indoor space, we set the maximum range of our radar to 4.01 m. The subsequent sampling frequency was 68 Hz. According to Nyquist theorem, we should be able to detect oscillations up to half of that frequency, making the fastest frequency we can detect 34 Hz. In addition to the radar's limitations, there are also tag limitations. As the oscillation frequency of a pendulum based tag depends solely on its arm length, there is a practical lower bound on the frequency a tag can have. For example, if we take the longest practical tag to be 12 cm that puts the lower bound for frequencies around 1.4 Hz. Now that we have a lower and upper bound, we need to investigate the smallest frequency difference that can be detected by the system. For this purpose, we conducted a quick experiment using the same simple harmonic pendulum oscillator used in the proof of concept Experiment 2. We used two different pendulum oscillators with string lengths of 10 cm and 10.67 cm respectively. Both oscillators were placed at the same distance, around one meter, from the radars. Both were interacted with 10 times with each interaction lasting around 10 seconds. Using the equation $T = 2\pi\sqrt{\frac{l}{g}}$, we calculate the frequency by taking the inverse of the time period. We found the corresponding frequencies to be 3 rpm or 0.05 Hz apart. The instances of both frequencies were able to be distinguished with a mean F1 score of 0.85 using the machine learning classifier.

With this empirical bound on minimum frequency resolution, we were able to calculate the number of oscillators for any given arm/string length constraints. With the help of equation $L = \frac{g}{(2\pi f)^2}$, we found the arm lengths between 2 cm and 12 cm that are at least 0.05 Hz apart. We found that a total of 42 distinguishable oscillators can be made as depicted in Figure 12. This is a reasonable amount for use in indoor environments when tagging everyday objects. As the equation suggests,

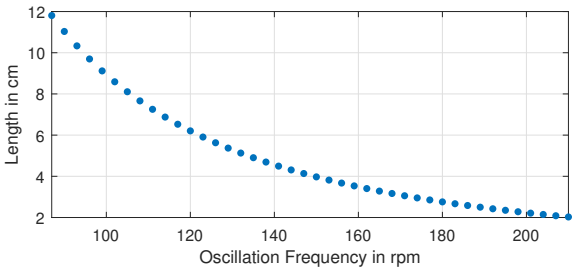

Figure 12. Frequency vs string length.

the arm length is inversely proportional to the square of the oscillation frequency, this allows us to have more tags with smaller arm lengths. For instance, if we decrease the upper limit of our allowable arm length by half, to 6 cm, we can still make 30 oscillators with a difference of 0.05 Hz (3 rpm). It is also important to note that tags with the same frequency could likely be used in multiple places in the same environment as the machine learning pipeline may be able to leverage location information to distinguish them.

REAL WORLD DEPLOYMENT WITH STATIONARY TAGS

Experimental Protocol

To test MechanoBeat in a real world scenario, we deployed MechanoBeat tags in a kitchen environment. We outfitted a drawer, cabinet, freezer, refrigerator, microwave, and countertop with pendulum and spring-mass based tags. Each tag has a unique oscillation frequency which was achieved by varying the arm length (i.e., 40, 60, 70, 80, and 100 mm) and spring-mass weight. One UWB radar box was placed on the stove-side wall and a second radar box was placed on the wall opposite to the kitchen hallway. Both radars were placed a distance of at least one meter away from the closest tag. The location of each tag and UWB radar boxes can be seen in Figure 13. Figure 14(a-c) shows how each pendulum-based tag was attached to a given appliance, cabinet or drawer. Figure 14(d) shows a condiment storage rack instrumented with a spring-mass-based tag and a magnetic reset mechanism.

All tags were attached to a stationary part of their corresponding appliance. Each tag was activated when its application door was opened, or in the drawers' case when the drawer was pulled out. Opening an application's door releases the oscillator arm, thus activating the tag. After the interaction is over we have a reset mechanism to stop oscillation. When the cabinet/drawer is closed the oscillator arm is held in place by the door/drawer. The freezer and refrigerator use a secondary part called a reset arm which attaches to the freezer/refrigerator door. When the door is closed, the piece holds the pendulum up so it cannot swing. When the condiment is taken away from the rack, the spring-mass oscillation is activated for a period of time until it dies out. As soon as the condiment bottle is replaced in the rack, a magnet attached to the bottom of the bottle attracts the mass back to its initial position.

Each experiment started with 10 seconds in which no tag was active. Then the tagged appliances were interacted with for 10 rounds. Interaction with the appliances involves opening and closing the appliance door. On average, the interaction duration (time span between opening and closing) was approximately 10 seconds. We refer to each round of appliance interaction as a cycle, i.e. collecting 10 cycles of data means 10 independent interactions with that appliance. We recorded the start time, end time, tag location, and interaction time for each cycle so that we have ground truth data for use in evaluation and training of the tag activation detection and classification model.

Tag Detection and Classification

We fine tuned a 1D CNN that had been pre-trained on data collected from Experiment 4. The multi-range bin model was trained from scratch. In order to incorporate data from both radars in our model, we average the concatenated single range bin embeddings before passing them to the multi-range bin model. We used a three second time window with a one second shift to convert our continuous time series data to discrete instances which we provide to our model. For each instance, we provided the model with range bins starting at the tag location minus 50 and ending at the tag location plus 50.

When training the entire pipeline we used leave-one-cycle-out cross-validation, wherein one cycle from each tag was held out for testing and another cycle held out for validation. All other cycles were used for training. We calculated the confusion matrix for each held out test cycle and summed all confusion matrices to get the results in Figure 17.

Our results show that MechanoBeat is able to accurately differentiate the various tags despite their close proximity to one another. Additionally, MechanoBeat is able to distinguish between no tag and tags with good accuracy. It is important to keep in mind that there is some lag between when a participant is instructed to start and end an interaction with an appliance and when the interaction actually starts and stops. As such, some instances that we labeled as no tag may have contained an active tag and vice versa. Thus what is more important than the absolute accuracy compared with our ground truth is that for each instance MechanoBeat is able to detect the correct tag and shows no tag before and after the instance. We demonstrate this characteristic for a single recording in Figure 16 in which our system is able to infer the correct tag at the right moment and has instances of no tag between each sequence attributed to a tag. As the figure shows there is generally a slight decrease in the probability of the tag towards the end of the active period, we attribute this to the decreasing displacement of the oscillating tag arm over time. This is supported by Experiment 5 where we show our model has reduced accuracy at sub millimeter-level displacements.

Multiple Tag Classification

We designed this experiment to investigate the accuracy of our system when two objects are interacted with at the same time. For instance, one can take an item from refrigerator to microwave while keeping the refrigerator door open. In order to create such interactions, two kitchen appliances were interacted with one after another with minimal transition time. Each combination of tag interactions was performed for 10 cycles. Our 1D CNN model trained only on previously collected single tag data was used to classify tags in the multiple

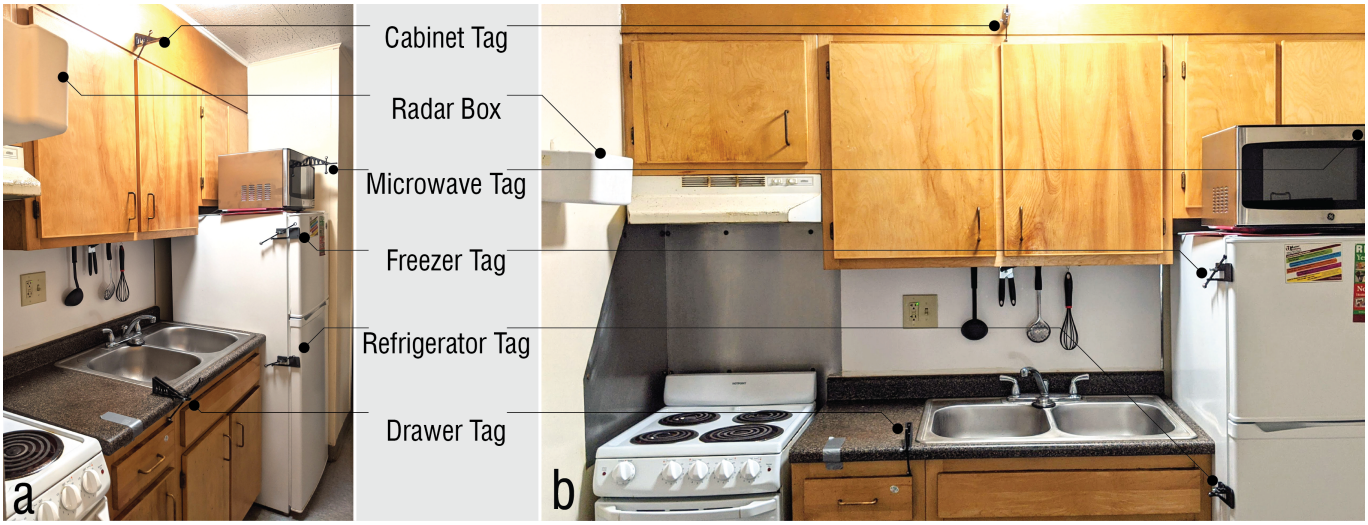

Figure 13. (a) Side view and (b) front view of the kitchen with instrumented pendulum based tags.

activation setting. Our model can reasonably detect such interactions and can identify which tags were interacted with an F1 score of 0.93.

Through Wall Sensing

In the real world, it is not always convenient or possible for a radar box to have a clear view of a given tag. Obstructions are common in indoor environments and can include walls, furniture, and people. In order to show MechanoBeat is robust to such occlusions we conducted the stationary tag experiment in an NLOS scenario. To simulate a non-line-of-sight situation

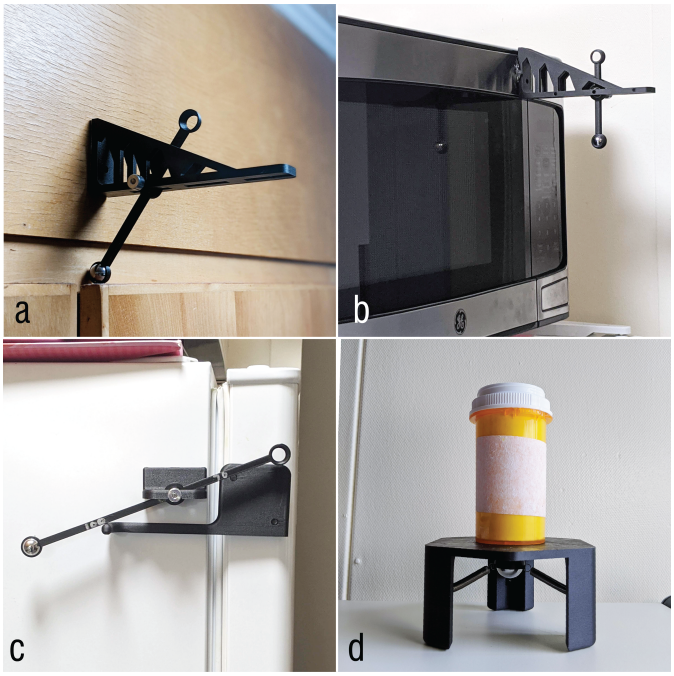

Figure 14. The (a) cabinet, (b) microwave, and (c) refrigerator are instrumented with pendulum based tags. (d) A condiment bottle is instrumented with a linear spring-mass tag.

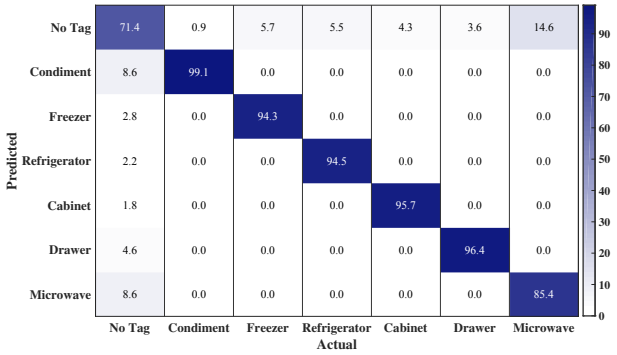

Figure 15. Confusion matrix for the stationary kitchen tags.

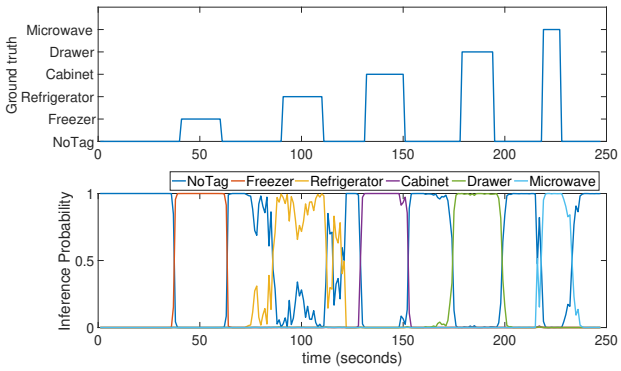

Figure 16. illustrates a sample recording.

we placed the radar boxes behind 9 inches of material similar to that used in home walls. The NLOS scenario was conducted in an identical fashion to the line-of-sight scenario except for the added material. The confusion matrix for the non-line-of-sight scenario can be seen in Figure 17. The recall, precision, and F1 score for both the line-of-sight and non-line-of-sight scenarios can be seen in Table 5. We can see that in the NLOS

Settings	R	P	F1
Line-of-sight	0.89	0.91	0.90
Through Wall	0.87	0.93	0.90

Table 5. The model performance in line-of-sight and non-line-of-sight (i.e., through wall) settings. The model performance was measured in terms of recall (R), precision (P) and F1 score.

scenario MechanoBeat performs similarly well to the line-of-sight scenario, which indicates our system is capable even when obstructed.

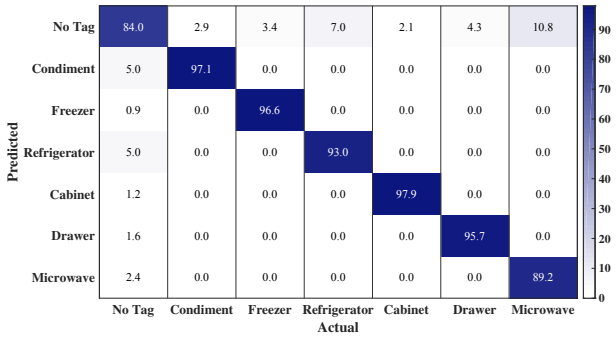

Figure 17. Confusion matrix for the stationary kitchen tags in a NLOS scenario.

MOBILE TAG EXPERIMENTS

Stationary MechanoBeat tags have a wide range of potential uses, but they are limited to a static location which may hinder some potential utilizations. In this section, we explore the design and results of a mobile MechanoBeat tag. We attach a mobile tag to a pill bottle to test one of the likely applications of such a tag. Tag oscillation is triggered when the lid of the pill bottle is twisted open. This oscillation can then be detected by the UWB radar and machine learning pipeline. Figures 1b and 3 show the prototype mobile tag design.

In our experiment, a pill bottle tag is held in the participant's hand while walking to four different chairs located in various locations within a $3m \times 3.5m$ space. Participants began by walking from a designated starting point to chair 1 while holding the pill bottle. While seated, the participant opened the pill bottle starting the tourbillon's oscillation which continued for approximately 10 seconds. Next, an activity simulating drinking water from a cup (available near the chair) was performed to create a realistic medicine intake event. The same protocol was maintained for the rest of the chairs/locations sequentially from chair 2 through chair 4. The entire event was repeated 10 times.

The Mechanobeat sensor received strong reflections from the moving body of the participant as well as the subtle motions from the tag's oscillation. Leveraging two UWB radars placed at two adjacent walls in the room we can track the movement of a user by applying a standard localization algorithm. For a detailed description, please refer to [37, 2, 40, 15]. Figure 18 illustrates the motion trajectory of a person in the room superimposed with the locations where the pill bottle tag was activated. The MechanoBeat system is able to localize and track the user in the room from the starting position to each of the chair's locations accurately. The inferred trajectory also matches the ground truth (green dash line) well. Moreover, the pill bottle interactions were correctly detected at locations near to the chair locations. Figure 19 shows the model's probability that the mobile tag is active against the ground truth, which clearly shows the models capability to distinguish active tag instances from non-active instances in the presence of moderate level of external body motion. By fusing the tag activation and location information, the MechanoBeat system can not only find when a mobile tag has been activated, but also its location in space.

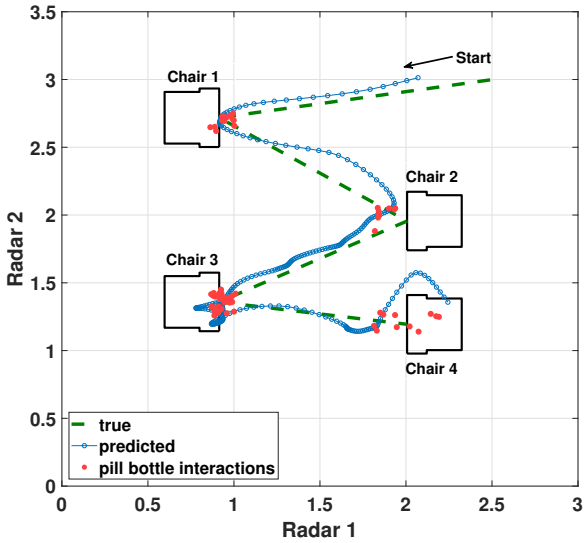

Figure 18. Movement trajectory predicted with the MechanoBeat system.

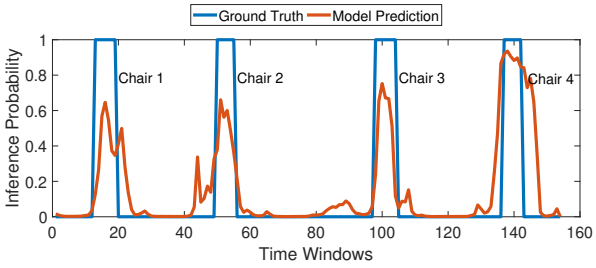

Figure 19. Probability that mobile tag is active over time.

SUPPLEMENTAL STUDY

Another application for our object interaction algorithm is to detect the flow from a water faucet. Our goal was to detect interactions with the faucet lever by finding the approximate water flow rate, namely: no flow, low flow, and high flow. For this purpose, we designed a 3D printed water-flow meter as shown in Figure 20. When any or both of the faucet levers (cold and/or hot) were turned on, water flowed through the meter causing its blades to rotate which could be detected by the UWB radar. The rotation frequency of the water flow meter depends on the flow rate of water coming from the tap,

thus the approximate amount of water flow can be found with our classification model.

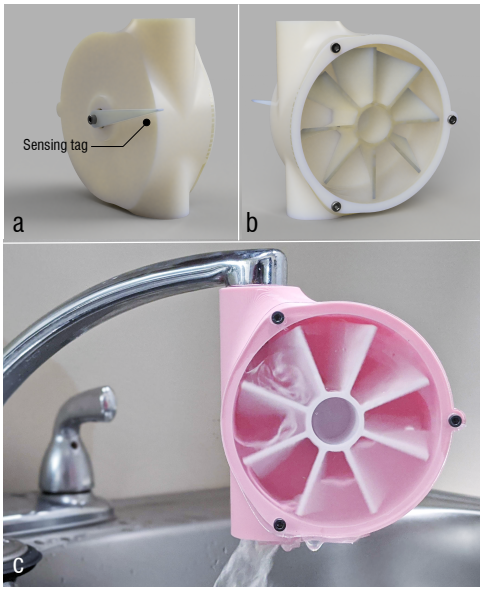

Figure 20. (a, b) Printed water flow-meter with rotary tag. (c) Water flow-meter in action.

In our experiment, the faucet levers were interacted with 10 times for both low and high flow. Low flow was activated by turning on one of the faucet levers, while high flow was activated by turning both on. Each interaction included opening the tap and letting the water run for 20 seconds before closing the tap. After running our deep learning classification algorithm with leave-one-cycle-out cross-validation, we were able to detect the three different states of flow with a mean F1 score of 0.9.

DISCUSSION, LIMITATIONS, AND FUTURE WORK

We present Mechanobeat, a system that employs: electronics-free tags that can be used to instrument everyday objects, a UWB radar array, and a novel sensing technique that leverages a 1D CNN classification model. We have shown that MechanoBeat fills a void in existing activity recognition and object interaction systems. Unlike other systems, MechanoBeat is capable of detecting tag activation without line-of-sight and shows strong performance even with non-static tags. In addition, we have designed various oscillation tags that can be made with common and affordable materials.

Furthermore, we have explored the limits of oscillation based tags and found that the classification accuracy fell when oscillation displacement was smaller than one millimeter. This finding opens the possibility for smaller tags and potentially totally new tag implementations.

As a working prototype, our tag designs are relatively large in size. However, we have created a smaller version of the pendulum based tag reducing the size by half. With an arm length of 38 mm including a metallic ball with a 6.35 mm diameter, as shown on the right side of Figure 21(a), we were able to successfully detect the interactions with a mean F1 score of 0.95. Figure 21(b), shows the confusion matrix of the smaller tag attached to the freezer.

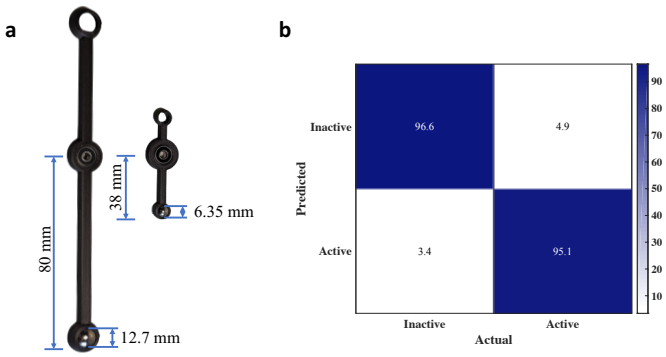

Figure 21. (a) Smaller version of a tag compared to a large tag. (b) Confusion matrix for detecting smaller tag.

We have tested MechanoBeat in a kitchen environment with two radars and multiple tags. However, more experiments can be conducted to better understand how MechanoBeat performs in complex scenarios such as environments with multiple people interacting with multiple tags. The tags were kept on their respective stationary appliances for a few months to simulate everyday use, in that period the tags produced the same oscillation frequencies throughout. A long-term deployment of MechanoBeat could further validate our system against mechanical wear and tear and allow us to examine the durability of our system over an extended time frame. Such a deployment would also provide us with additional data, which could be used to train our detection model, further improving accuracy.

CONCLUSION

We have developed cheap electronics-free tags, that use harmonic oscillation to produce unique frequencies when interacted with. We have demonstrated how these tags can be deployed to monitor object and environmental interactions in a real world setting. Using our proposed signal processing pipeline and deep learning algorithm, we are successful in detecting tag oscillation in both line-of-sight and non-line-of-sight scenarios. Furthermore, our sensing approach uses only RF reflections from the tag oscillation captured by UWB radar without the need for additional information.

ACKNOWLEDGMENTS

We sincerely thank the reviewers for their insightful comments and suggestions that helped to improve the paper. This work is in part supported by the National Science Foundation under grant SBE 1839999 and start up grant support from College of Information and Computer Sciences and the Institute for Applied Life Sciences at the University of Massachusetts Amherst.

REFERENCES

[1] 2015. PulsON 440 UWB Radar. (2015). `https://fccid.io/NUF-P440-A/User-Manual/User-Manual-287844`.

[2] Fawzy Abujarad, Andreas Jostingmeier, and AS Omar. 2004. Clutter removal for landmine using different signal processing techniques. In *Proceedings of the*

Tenth International Conference on Grounds Penetrating Radar, 2004. GPR 2004. IEEE, 697–700.

[3] Fadel Adib, Zach Kabelac, Dina Katabi, and Robert C. Miller. 2014. 3D Tracking via Body Radio Reflections. In *Proceedings of the 11th USENIX Symposium on Networked Systems Design and Implementation (NSDI 14)*. USENIX Association, Seattle, WA, 317–329. https://www.usenix.org/conference/nsdi14/technical-sessions/presentation/adib

[4] Fadel Adib and Dina Katabi. 2013. See through Walls with WiFi!. In *Proceedings of the ACM SIGCOMM 2013 Conference on SIGCOMM (SIGCOMM '13)*. Association for Computing Machinery, New York, NY, USA, 75–86. DOI: http://dx.doi.org/10.1145/2486001.2486039

[5] Bosch. 2020. XDK Cross Domain Development Kit. (2020). https://www.bosch-connectivity.com/products/cross-domain/cross-domain-developement-kit/ accessed March 13, 2020.

[6] Michael Buettner, Richa Prasad, Alanson Sample, Daniel Yeager, Ben Greenstein, Joshua R. Smith, and David Wetherall. 2008. RFID Sensor Networks with the Intel WISP. In *Proceedings of the 6th ACM Conference on Embedded Network Sensor Systems (SenSys '08)*. Association for Computing Machinery, New York, NY, USA, 393–394. DOI: http://dx.doi.org/10.1145/1460412.1460468

[7] Jeong Woo Choi, Dae Hyeon Yim, and Sung Ho Cho. 2017. People counting based on an IR-UWB radar sensor. *IEEE Sensors Journal* 17, 17 (2017), 5717–5727. DOI:http://dx.doi.org/10.1109/JSEN.2017.2723766

[8] Gabe Cohn, Sidhant Gupta, Jon Froehlich, Eric Larson, and Shwetak N. Patel. 2010a. GasSense: Appliance-level, Single-point Sensing of Gas Activity in the Home. In *Proceedings of the 8th International Conference on Pervasive Computing (Pervasive'10)*. Springer-Verlag, Berlin, Heidelberg, 265–282. DOI: http://dx.doi.org/10.1007/978-3-642-12654-3_16

[9] Gabe Cohn, Erich Stuntebeck, Jagdish Pandey, Brian Otis, Gregory D. Abowd, and Shwetak N. Patel. 2010b. SNUPI: Sensor Nodes Utilizing Powerline Infrastructure. In *Proceedings of the 12th ACM International Conference on Ubiquitous Computing (UbiComp '10)*. ACM, New York, NY, USA, 159–168. DOI:http://dx.doi.org/10.1145/1864349.1864377

[10] Abe Davis, Michael Rubinstein, Neal Wadhwa, Gautham J. Mysore, Frédo Durand, and William T. Freeman. 2014. The Visual Microphone: Passive Recovery of Sound from Video. *ACM Trans. Graph.* 33, 4, Article 79 (July 2014), 10 pages. DOI: http://dx.doi.org/10.1145/2601097.2601119

[11] Samuel DeBruin, Branden Ghena, Ye-Sheng Kuo, and Prabal Dutta. 2015. PowerBlade: A Low-Profile, True-Power, Plug-Through Energy Meter. 17–29. DOI: http://dx.doi.org/10.1145/2809695.2809716

[12] A. Figueroa, B. Al-Qudsi, N. Joram, and F. Ellinger. 2016. Comparison of two-way ranging with FMCW and UWB radar systems. In *Proceedings of the 2016 13th Workshop on Positioning, Navigation and Communications (WPNC)*. 1–6. DOI: http://dx.doi.org/10.1109/WPNC.2016.7822856

[13] James Fogarty, Carolyn Au, and Scott E. Hudson. 2006. Sensing from the Basement: A Feasibility Study of Unobtrusive and Low-Cost Home Activity Recognition. In *Proceedings of the 19th Annual ACM Symposium on User Interface Software and Technology (UIST '06)*. Association for Computing Machinery, New York, NY, USA, 91–100. DOI: http://dx.doi.org/10.1145/1166253.1166269

[14] Jon E. Froehlich, Eric Larson, Tim Campbell, Conor Haggerty, James Fogarty, and Shwetak N. Patel. 2009. HydroSense: Infrastructure-Mediated Single-Point Sensing of Whole-Home Water Activity. In *Proceedings of the 11th International Conference on Ubiquitous Computing (UbiComp '09)*. Association for Computing Machinery, New York, NY, USA, 235–244. DOI: http://dx.doi.org/10.1145/1620545.1620581

[15] Charlotte E Goldfine, Md Farhan Tasnim Oshim, Stephanie P Carreiro, Brittany P Chapman, Deepak Ganesan, and Tauhidur Rahman. 2020. Respiratory Rate Monitoring in Clinical Environments with a Contactless Ultra-Wideband Impulse Radar-based Sensor System. In *Proceedings of the 53rd Hawaii International Conference on System Sciences*, Vol. 2020. 3366. DOI: http://dx.doi.org/10.24251/HICSS.2020.412

[16] Berk Gulmezoglu, Mehmet Burak Guldogan, and Sinan Gezici. 2014. Multiperson tracking with a network of ultrawideband radar sensors based on Gaussian mixture PHD filters. *IEEE Sensors Journal* 15, 4 (2014), 2227–2237. DOI: http://dx.doi.org/10.1109/JSEN.2014.2372312

[17] Sidhant Gupta, Matthew S. Reynolds, and Shwetak N. Patel. 2010. ElectriSense: Single-point Sensing Using EMI for Electrical Event Detection and Classification in the Home. In *Proceedings of the 12th ACM International Conference on Ubiquitous Computing (UbiComp '10)*. ACM, New York, NY, USA, 139–148. DOI:http://dx.doi.org/10.1145/1864349.1864375

[18] Texas Instruments. 2015. SimpleLink multi-standard CC2650 SensorTag. (2015). http://www.ti.com/tool/TIDC-CC2650STK-SENSORTAG accessed March 13, 2020.

[19] Vikram Iyer, Justin Chan, and Shyamnath Gollakota. 2017. 3D Printing Wireless Connected Objects. *ACM Trans. Graph.* 36, 6, Article 242 (Nov. 2017), 13 pages. DOI:http://dx.doi.org/10.1145/3130800.3130822

[20] Faheem Khan, Seong Kyu Leem, and Sung Ho Cho. 2017. Hand-Based Gesture Recognition for Vehicular Applications Using IR-UWB Radar. *Sensors* 17, 4 (2017). DOI:http://dx.doi.org/10.3390/s17040833

[21] Gierad Laput, Walter S. Lasecki, Jason Wiese, Robert Xiao, Jeffrey P. Bigham, and Chris Harrison. 2015. Zensors: Adaptive, Rapidly Deployable, Human-Intelligent Sensor Feeds. In *Proceedings of the 33rd Annual ACM Conference on Human Factors in Computing Systems (CHI '15)*. Association for Computing Machinery, New York, NY, USA, 1935–1944. DOI: http://dx.doi.org/10.1145/2702123.2702416

[22] Gierad Laput, Robert Xiao, and Chris Harrison. 2016. ViBand: High-Fidelity Bio-Acoustic Sensing Using Commodity Smartwatch Accelerometers. In *Proceedings of the 29th Annual Symposium on User Interface Software and Technology (UIST '16)*. Association for Computing Machinery, New York, NY, USA, 321–333. DOI: http://dx.doi.org/10.1145/2984511.2984582

[23] Gierad Laput, Yang Zhang, and Chris Harrison. 2017. Synthetic Sensors: Towards General-Purpose Sensing. In *Proceedings of the 2017 CHI Conference on Human Factors in Computing Systems (CHI '17)*. Association for Computing Machinery, New York, NY, USA, 3986–3999. DOI: http://dx.doi.org/10.1145/3025453.3025773

[24] Seong Kyu Leem, Faheem Khan, and Sung Ho Cho. 2017. Vital Sign Monitoring and Mobile Phone Usage Detection Using IR-UWB Radar for Intended Use in Car Crash Prevention. *Sensors* 17, 6 (2017). DOI: http://dx.doi.org/10.3390/s17061240

[25] Dingzeyu Li, Avinash S. Nair, Shree K. Nayar, and Changxi Zheng. 2017. AirCode: Unobtrusive Physical Tags for Digital Fabrication. In *Proceedings of the 30th Annual ACM Symposium on User Interface Software and Technology (UIST '17)*. Association for Computing Machinery, New York, NY, USA, 449–460. DOI: http://dx.doi.org/10.1145/3126594.3126635

[26] Ce Liu, Antonio Torralba, William T. Freeman, Frédo Durand, and Edward H. Adelson. 2005. Motion Magnification. *ACM Trans. Graph.* 24, 3 (July 2005), 519–526. DOI: http://dx.doi.org/10.1145/1073204.1073223

[27] Emmanuel Munguia Tapia, Stephen S. Intille, and Kent Larson. 2007. Portable Wireless Sensors for Object Usage Sensing in the Home: Challenges and Practicalities. In *European Conference on Ambient Intelligence*, Bernt Schiele, Anind K. Dey, Hans Gellersen, Boris de Ruyter, Manfred Tscheligi, Reiner Wichert, Emile Aarts, and Alejandro Buchmann (Eds.). Springer Berlin Heidelberg, Berlin, Heidelberg, 19–37. DOI:http://dx.doi.org/10.1007/978-3-540-76652-0_2

[28] Admir Muric, Christos Anestis Georgiadis, Fisayo Caleb Sangogboye, and Mikkel Baun Kjærgaard. 2019. Practical IR-UWB-Based Occupant Counting Evaluated in Multiple Field Settings. In *Proceedings of the 1st ACM International Workshop on Device-Free Human Sensing (DFHS'19)*. Association for Computing Machinery, New York, NY, USA, 48–51. DOI: http://dx.doi.org/10.1145/3360773.3360885

[29] Notion. 2020. Notion Sensors. (2020). https://getnotion.com/products/notion-sensors accessed March 13, 2020.

[30] Katsunori Ohnishi, Atsushi Kanehira, Asako Kanezaki, and Tatsuya Harada. 2016. Recognizing activities of daily living with a wrist-mounted camera. In *Proceedings of the IEEE Conference on Computer Vision and Pattern Recognition*. 3103–3111. DOI: http://dx.doi.org/10.1109/CVPR.2016.338

[31] Shwetak N. Patel, Matthew S. Reynolds, and Gregory D. Abowd. 2008. Detecting Human Movement by Differential Air Pressure Sensing in HVAC System Ductwork: An Exploration in Infrastructure Mediated Sensing. In *Proceedings of the International Conference on Pervasive Computing*, Jadwiga Indulska, Donald J. Patterson, Tom Rodden, and Max Ott (Eds.). Springer Berlin Heidelberg, Berlin, Heidelberg, 1–18.

[32] Shwetak N. Patel, Thomas Robertson, Julie A. Kientz, Matthew S. Reynolds, and Gregory D. Abowd. 2007. At the Flick of a Switch: Detecting and Classifying Unique Electrical Events on the Residential Power Line. In *Proceedings of the 9th International Conference on Ubiquitous Computing (UbiComp '07)*. Springer-Verlag, Berlin, Heidelberg, 271–288. http://dl.acm.org/citation.cfm?id=1771592.1771608

[33] Matthai Philipose, Kenneth P. Fishkin, Mike Perkowitz, Donald J. Patterson, Dieter Fox, Henry Kautz, and Dirk Hahnel. 2004. Inferring Activities from Interactions with Objects. *IEEE Pervasive Computing* 3, 4 (Oct. 2004), 50–57. DOI:http://dx.doi.org/10.1109/MPRV.2004.7

[34] Tauhidur Rahman, Alexander T. Adams, Ruth Vinisha Ravichandran, Mi Zhang, Shwetak N. Patel, Julie A. Kientz, and Tanzeem Choudhury. 2015. DoppleSleep: A Contactless Unobtrusive Sleep Sensing System Using Short-range Doppler Radar. In *Proceedings of the 2015 ACM International Joint Conference on Pervasive and Ubiquitous Computing (UbiComp '15)*. ACM, New York, NY, USA, 39–50. DOI: http://dx.doi.org/10.1145/2750858.2804280

[35] Bernd Schleicher, Ismail Nasr, Andreas Trasser, and Hermann Schumacher. 2013. IR-UWB radar demonstrator for ultra-fine movement detection and vital-sign monitoring. *IEEE transactions on microwave theory and techniques* 61, 5 (2013), 2076–2085. DOI: http://dx.doi.org/10.1109/TMTT.2013.2252185

[36] Joshua R. Smith, Alanson P. Sample, Pauline S. Powledge, Sumit Roy, and Alexander Mamishev. 2006. A Wirelessly-Powered Platform for Sensing and Computation. In *Proceedings of the 8th International Conference on Ubiquitous Computing (UbiComp'06)*. Springer-Verlag, Berlin, Heidelberg, 495–506. DOI: http://dx.doi.org/10.1007/11853565_29

[37] Fok Hing Chi Tivive, Abdesselam Bouzerdoum, and Moeness G Amin. 2011. An SVD-based approach for mitigating wall reflections in through-the-wall radar imaging. In *2011 IEEE RadarCon (RADAR)*. IEEE, 519–524. DOI: http://dx.doi.org/10.1109/RADAR.2011.5960591

[38] Karl D. D. Willis and Andrew D. Wilson. 2013. InfraStructs: Fabricating Information inside Physical Objects for Imaging in the Terahertz Region. *ACM Trans. Graph.* 32, 4, Article Article 138 (July 2013), 10 pages. DOI:http://dx.doi.org/10.1145/2461912.2461936

[39] Yunqiang Yang and Aly E Fathy. 2005. See-through-wall imaging using ultra wideband short-pulse radar system. In *2005 IEEE Antennas and Propagation Society International Symposium*, Vol. 3. IEEE, 334–337. DOI: http://dx.doi.org/0.1109/APS.2005.1552508

[40] Rudolf Zetik, Stephen Crabbe, Jozef Krajnak, Peter Peyerl, Jürgen Sachs, and Reiner Thomä. 2006. Detection and localization of persons behind obstacles using M-sequence through-the-wall radar. In *Sensors, and Command, Control, Communications, and Intelligence (C3I) Technologies for Homeland Security and Homeland Defense V*, Edward M. Carapezza (Ed.), Vol. 6201. International Society for Optics and Photonics, SPIE, 145 – 156. DOI: http://dx.doi.org/10.1117/12.667989

[41] Cemin Zhang, Michael Kuhn, Brandon Merkl, Aly E Fathy, and Mohamed Mahfouz. 2006. Accurate UWB indoor localization system utilizing time difference of arrival approach. In *2006 IEEE radio and wireless symposium*. IEEE, 515–518. DOI: http://dx.doi.org/10.1109/RWS.2006.1615207

[42] Daqiang Zhang, Jingyu Zhou, Minyi Guo, Jiannong Cao, and Tianbao Li. 2010. TASA: Tag-free activity sensing using RFID tag arrays. *IEEE Transactions on Parallel and Distributed Systems* 22, 4 (2010), 558–570. DOI: http://dx.doi.org/10.1109/TPDS.2010.118

[43] Yang Zhang, Yasha Iravantchi, Haojian Jin, Swarun Kumar, and Chris Harrison. 2019. Sozu: Self-Powered Radio Tags for Building-Scale Activity Sensing. In *Proceedings of the 32nd Annual ACM Symposium on User Interface Software and Technology (UIST '19)*. Association for Computing Machinery, New York, NY, USA, 973–985. DOI: http://dx.doi.org/10.1145/3332165.3347952

[44] Yang Zhang, Gierad Laput, and Chris Harrison. 2018a. Vibrosight: Long-Range Vibrometry for Smart Environment Sensing. In *Proceedings of the 31st Annual ACM Symposium on User Interface Software and Technology (UIST '18)*. Association for Computing Machinery, New York, NY, USA, 225–236. DOI: http://dx.doi.org/10.1145/3242587.3242608

[45] Yang Zhang, Chouchang (Jack) Yang, Scott E. Hudson, Chris Harrison, and Alanson Sample. 2018b. Wall++: Room-Scale Interactive and Context-Aware Sensing. In *Proceedings of the 2018 CHI Conference on Human Factors in Computing Systems (CHI '18)*. Association for Computing Machinery, New York, NY, USA, 1–15. DOI:http://dx.doi.org/10.1145/3173574.3173847

[46] Chen Zhao, Sam Yisrael, Joshua R. Smith, and Shwetak N. Patel. 2014. Powering Wireless Sensor Nodes with Ambient Temperature Changes. In *Proceedings of the 2014 ACM International Joint Conference on Pervasive and Ubiquitous Computing (UbiComp '14)*. ACM, New York, NY, USA, 383–387. DOI:http://dx.doi.org/10.1145/2632048.2632066

[47] Mingmin Zhao, Tianhong Li, Mohammad Abu Alsheikh, Yonglong Tian, Hang Zhao, Antonio Torralba, and Dina Katabi. 2018. Through-Wall Human Pose Estimation Using Radio Signals. In *Proceedings of the IEEE Computer Society Conference on Computer Vision and Pattern Recognition (Proceedings of the IEEE Computer Society Conference on Computer Vision and Pattern Recognition)*. IEEE, Institute of Electrical and Electronics Engineers, United States, 7356–7365. DOI: http://dx.doi.org/10.1109/CVPR.2018.00768